Crystallization of Poly(Ethylene Terephthalate) (PET) from the Oriented Mesomorphic Form

LIDIA PARRAVICINI,[1] BIAGIO LEONE,[1] FINIZIA AURIEMMA,[1] GAETANO GUERRA,[1,*] VITTORIO PETRACCONE,[1] GABRIELE DI DINO,[2] RICCARDO BIANCHI,[2] and RENATO VOSA[2]

[1]Dipartimento di Chimica, Universita' di Napoli Federico II, via Mezzocannone 4, I-80134, Naples, Italy and [2]Centro Ricerche Montefibre, I-80011, Acerra, Naples, Italy

SYNOPSIS

Yarns of different inherent viscosities, in the range 0.6–1.1 dL/g, spun in industrial plants, and drawn at room temperature to obtain mesomorphic samples, have been characterized. The evolution from the mesomorphic form toward the triclinic crystalline form has also been studied by combined differential scanning calorimetry (DSC), dynamic mechanical analyses (DMA), and accurate wide angle X-ray diffraction experiments. The DMA analysis of the mesomorphic samples allows better resolution of the glass transition and crystallization phenomena, which are superimposed in the DSC scans. The degree of molecular orientation in the mesomorphic samples, and the temperature of crystallization from the mesomorphic form (60–80°C), are essentially independent of the polymer molar mass.

INTRODUCTION

A mesomorphic form of poly(ethylene terephthalate) (PET) was found several years ago.[1–4] It can be obtained by drawing procedures on amorphous unoriented samples at temperatures below the glass transition (T_g), and it is transformed into the usual triclinic structure by heating above T_g.

X-ray diffraction patterns of this form present only sharp reflections on the meridian, with spacings in agreement with a periodicity of 10.3 Å,[4,5] which is different from the c periodicity (10.7 Å) that was observed for the usual triclinic form.[6,7] In addition to the meridional reflections, only a broad (with respect to both reciprocal coordinates ξ and ζ) scattering peak on the equator is present.[4]

The conformation and the packing of PET chains in the mesomorphic form have been investigated by X-ray diffraction measurements, conformational energy analysis, and calculation of Fourier transforms of models.[5] The reported Fourier transform calculations of isolated-chain models have indicated that the experimental diffraction pattern of the mesomorphic form of PET can be qualitatively accounted for by extended linear chains, obtained by random sequences of monomeric units in different minimum energy conformations. This indicates a substantial absence in the mesomorphic form of rotational (around the chain axis) and translational (along the chain axis) order between adjacent parallel chains. In particular, the energy and geometrical analyses have suggested that the different conformations of the monomeric unit, which would be present in the PET chain in the mesomorphic form, could be characterized by all nearly *trans* conformations, but for the C—O—C—C dihedral angles, for which, in addition to values close to 180°, values close to +80° and −80° would be possible.[5]

Low angle light scattering and optical microscopy have shown that the mesomorphic form, obtained by cold drawing, has a rod-like superstructure, in which the rods are preferentially oriented in the stretching direction[8]; the structure is presumed to be formed of extended chain crystallites.[8]

A large part of the processes described in the literature, for obtaining medium and high modulus and/or strength PET fibers, involves two successive drawing procedures, the first one being at temperatures below the glass transition.[9–16] In these low temperature drawing procedures, fibers in the me-

* To whom correspondence should be addressed.
Journal of Applied Polymer Science, Vol. 52, 875–885 (1994)
 CCC 0021-8995/94/070875-11

somorphic form can be obtained, which are fully crystallized only in the subsequent drawing procedures at higher temperatures (generally in the temperature range 170–250°C). In addition, this yields some technological relevance to the study of the crystallization of PET starting from the oriented mesomorphic form.

The evolution by annealing of the mesomorphic form of PET, toward the triclinic form, has been studied by photographic X-ray diffraction patterns by Asano and Seto.[4] In particular, the first appearance of the reflections of the triclinic form was observed for annealing at 80°C and a complete disappearance of the meridional (001) reflection, typical of the mesomorphic form, was observed only for annealing at temperatures close to or higher than 100°C.[4]

According to Misra and Stein,[8] annealing of cold drawn samples at constant length does not change the rodlike superstructure and the extended chain crystal structure, while free annealing produces chain-folded crystals.

Several studies by differential scanning calorimetry (DSC) for mesomorphic samples, although generally indicated as amorphous oriented samples, have been reported.[17-21] In particular, it has been shown that the well defined exothermic peaks of the amorphous samples (corresponding to the crystallization process) are substituted for the mesomorphic samples by a broad peak whose shape changes with drawing conditions (temperature, rate, and ratio).

In the present article, the evolution from the mesomorphic form toward the triclinic crystalline form has been followed, for yarns of different inherent viscosities spun in industrial plants, by combined differential scanning calorimetry, dynamic mechanical analyses (DMA), and accurate wide angle X-ray diffraction experiments (by an automatic diffractometer).

EXPERIMENTAL

Materials and Processing Conditions

The PET fibers were obtained by melt-spinning from pellets obtained by the dimethyl terephtalate process, with antimony as the polycondensation catalyst. The inherent viscosities of the polymer samples, η, determined at 35°C in *o*-chlorophenol are 0.6, 0.8, 0.9, and 1.1 dL/g, respectively; the diethylene glycol content for all the samples is close to 0.65 mol %.

The PET samples were extruded through a spinneret of 5 holes, yielding approximately the same linear density (180 g/10,000 m) independently of the molar mass. This corresponds to the diameters of the single filaments of nearly 60 μm. The fibers were collected at rotating drums at wind-up speeds of 60 m/min at a quench air temperature of 25°C.

Monofilaments of a larger section ($\approx$ 500 μm) were also prepared from the same polymers by a laboratory extruder and were collected at a wind-up speed of 45 m/min.

The process of drawing at room temperature for the fibers was performed on a Dynafil apparatus, with a draw ratio of 2.3 and a wind-up speed of 2.5 m/min. For the monofilaments, the drawing was performed in a Minimat apparatus of the Polymer Laboratories with a draw ratio of nearly 5 and a strain rate of 10%/min.

The annealing procedures on the drawn fibers and monofilaments were performed on bundles with fixed ends in the Minimat apparatus. The temperature control was ±1°C and the annealing time was 15 min.

Characterization Techniques

Humidity conditioning was achieved by storing the samples in a controlled temperature chamber with 65% relative humidity, maintained using a saturated NH_4Cl and KNO_3 solution. This corresponds to equilibrium moisture contents, for the as-spun fibers, of nearly 0.6%. The humidity conditioning is crucial for the measure of the crystallization temperature (T_c) from the glassy state.[22,23] In particular, T_c depends on the moisture content for values lower than 0.2%.[23]

The X-ray diffraction patterns for the oriented samples were obtained using a Nonius automatic X-ray diffractometer with Ni-filtered CuKα radiation, and were collected, always maintaining an equatorial geometry. In this article, only equatorial scans (along ξ for $\zeta = 0$), and azimuthal scans for $2\Theta \approx 26°$, around the meridional peak of the third layer line of the mesomorphic form (at $\xi = 0$ and $\zeta = 3/c$, with $c = 10.3$ Å), are reported. The measurements were performed on bundles of fibers that were maintained parallel in a Lyndemann capillary. For the equatorial scans, a subtraction of the diffraction halo of the capillary was necessary.

The birefringences were determined using a Leitz polarizing microscope with Ehringhaus rotary compensators of 5 orders for the as-spun fibers, and of 30 orders for the drawn fibers. To obtain the birefringence, measurements of the fiber diameters were

necessary. These measurements were made directly, using the optical microscope with a filar eyepiece. A stage micrometer was used to calibrate the filar eyepiece.

A Perkin–Elmer DSC-7 was used for the calorimetric analyses. DSC scans were obtained for heating rates in the range 10–80°C/min. The increase of the melting temperatures with the heating rate (of more than 10°C/min) indicates the prevalence of superheating phenomena with respect to possible recrystallization phenomena. As a consequence, we have preferred to report the data for the lowest considered heating rate (10°C/min). The fibers were cut into pieces of about 1–2 mm in length to minimize the effect of fiber shrinkage upon heating.[24] The average sample weight was about 8 mg, for the as-spun fibers, and was about 3 mg, for the drawn fibers.

The dynamic mechanical analysis was carried out with a Polymer Laboratories DMTA apparatus at a measurement frequency of 10 Hz and at a heating rate of 1°C/min. Bundles of fibers (nearly 150 filaments) have been mounted in the bending mode as a double cantilever. The incomplete parallelism of the filaments and the inaccuracy in the determination of the sample section, which is subjected to the bending, reduces the accuracy of the measured moduli. However, a fear accuracy is reached for the measurements of the loss factor tan δ. Qualitatively similar, but more accurate, DMA scans are obtained for the single thick monofilaments (diameters of nearly 500 μm). The reported scans for the moduli refer only to the thick monofilaments.

The mechanical tests at room temperature were performed on an Instron testing device. Single filaments were randomly chosen from a given fiber and ten specimens were tested in each experiment. The gauge length was 150 mm and the strain rate was 100%/min. The mechanical tests at 195°C were performed on a Minimat dynamometer with a gauge length of 5 mm and a strain rate of 200%/min.

RESULTS AND DISCUSSION

Amorphous Spun Fibers

As expected and confirmed by X-ray diffraction spectra, all the fibers, obtained by spinning in similar conditions of the four polymer samples of different inherent viscosities, were fully amorphous.

The DSC scans of these amorphous spun fibers are shown in Figure 1. While the positions of the specific heat (c_p) steps, typical of the glass transition and of the melting endothermic peaks, are substantially independent of the molar mass ($T_g \approx$ 82–84°C and $T_m \approx$ 253–254°C), the positions of the crystallization exothermic peaks are not. In particular, with increasing η, the crystallization peak temperature decreases regularly from 131°C to 123.5°C.

For all the considered spun fibers as well as the monofilaments, the general aspect of the DMA scans is essentially the same. A DMA scan, for monofilament (500 μm) with η = 0.6, is shown, for instance, in Figure 2. An intense tan δ peak, which corresponds to the large drop in the modulus of the glass

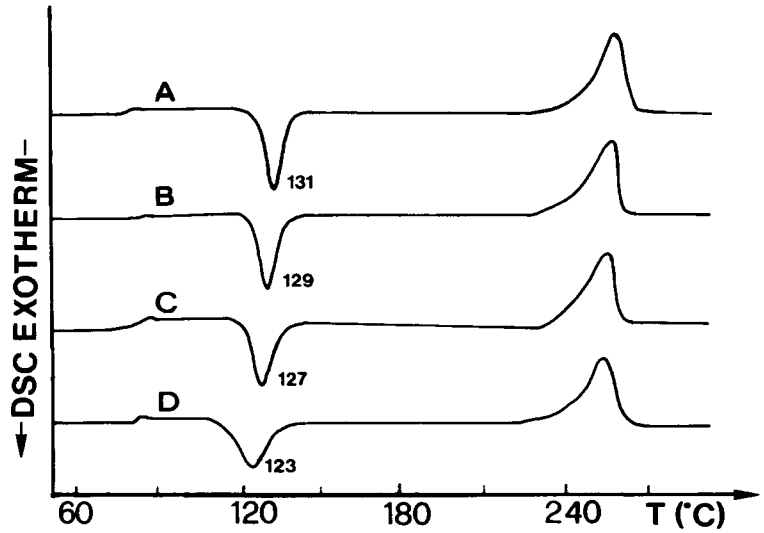

Figure 1 DSC scans, at the heating rate of 10°C/min, for the as-spun fibers of different inherent viscosities: (A) 0.6 dL/g, (B) 0.8 dL/g, (C) 0.9 dL/g, and (D) 1.1 dL/g. The temperatures, corresponding to the exothermic peaks, are indicated.

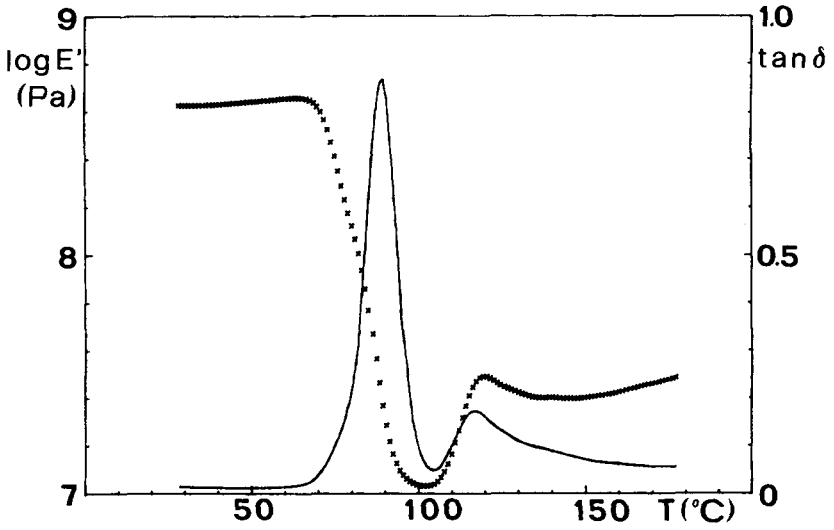

Figure 2 Storage modulus, E' (xxxx) and loss factor, tan δ (——), from dynamic mechanical measurements, at a frequency of 10 Hz and at a heating rate of 1°C/min, for the monofilament with η = 0.6 dL/g.

transition, is located at 88.5°C, while a smaller tan δ peak, corresponding to the increase of the elastic modulus associated with the crystallization phenomenon, is located at higher temperatures. Several DMA scans for amorphous PET samples (generally films) are reported in the literature,[11,25-32] which do not present the latter tan δ peak. The presence, for as spun PET years, of the high temperature tan δ peak, associated with the crystallization, was already reported, however, in an article where the measurements were continued up to 140°C.[33] This peak temperature decreases for the as-spun fibers with the molar mass, as shown by the enlarged details of the loss factor curves in Figure 3.

The temperatures of the DSC crystallization peaks (T_c^{DSC}) and of the higher temperature tan δ peaks (T_c^{DMA}) are plotted vs. the inherent viscosity in Figure 4. Both sets of data clearly indicate that

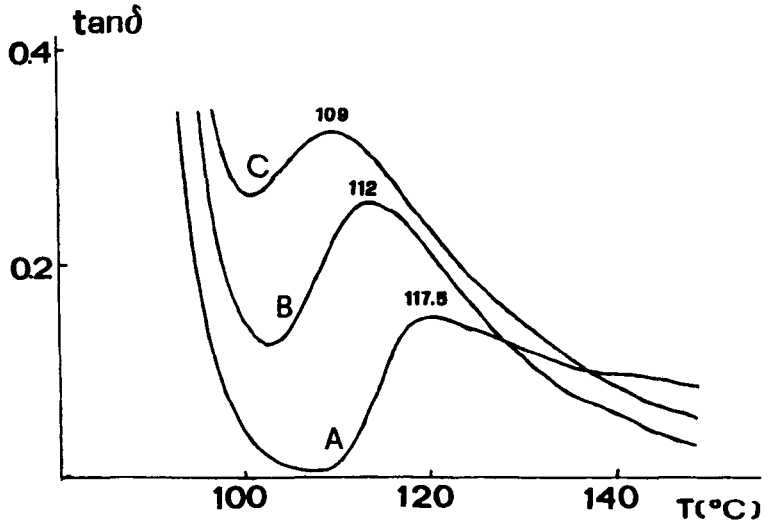

Figure 3 Detail of the loss factor (tan δ) curves, from dynamic mechanical scans similar to that shown in Figure 2, for the as-spun fibers of different inherent viscosities: (A) 0.6 dL/g, (B) 0.9 dL/g, and (C) 1.1 dL/g. For the clarity of the plot, the curve for the sample with η = 0.8 dL/g has been omitted, because it partially overlaps curve A. The temperatures, corresponding to the tan δ peaks, are indicated.

the crystallization from the amorphous phase occurs at lower temperatures (i.e., more easily) for samples of higher molar mass.

Let us recall that the opposite phenomenon has been observed for unoriented PET samples (e.g., increases of crystallization peak temperatures of nearly 8°C for an increase of η from 0.6 to 0.76 dL/g[22]). In addition, the rates of crystallization from the melt state are sensibly reduced for PET by increases of the molar mass, in the considered range.[34] Those decreases of the crystallization rates with increasing the molar mass are probably caused by the increases of viscosity and the corresponding decreases of the chain mobility.[34]

The reduction of T_c, that is, the increase of the crystallization rate, with increasing η, observed for our spun fibers (Fig. 4), is due to the fact that the viscosity effect, reducing the crystallization rate, is overcome by a molecular orientation effect that increases the crystallization rate.[35-37] In fact, although the spinning conditions are similar, the birefringences measured for spun fibers of higher molar mass are significantly increased (Fig. 4). Analogous variations of the birefringence with the inherent viscosity of PET samples have been described in the literature.[38]

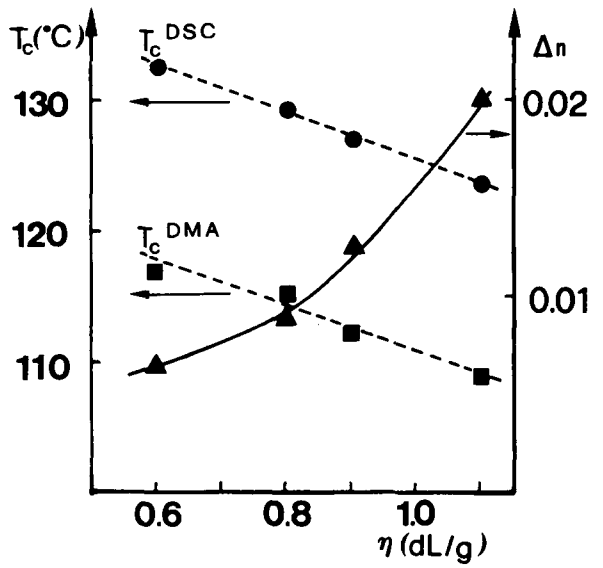

Figure 4 The temperatures of the DSC crystallization peaks (●, taken from Fig. 1) and of the higher temperature tan δ peaks (■, taken from Fig. 3) are plotted vs. the inherent viscosity. In addition, on the right scale the birefringences, measured for the as-spun fibers (▲), are reported.

Mesomorphic Fibers

The mechanical properties of the spun fibers, after drawing at room temperature, are markedly dependent on η. For instance, the tensile strength and modulus, measured at room temperature, increase regularly from 0.25 to 0.6 GPa and from 7 to 10 GPa, respectively (the breaking strain remains for all the fibers close to 35%). The strain at break, measured at 195°C (for the strain rate of 2 min^{-1}) also increases regularly from 1.2 to 1.6, corresponding to overall draw ratios (including also the draw ratio of the first drawing at room temperature) of 2.8 to 3.7, respectively. The increase of the drawability (the attainable maximum draw ratio) with increasing the molar mass of PET is described in the literature.[11]

Correspondingly, the X-ray diffraction patterns, the birefringence, and the DSC and DMA scans of the room temperature drawn fibers are instead poorly dependent on η.

In particular, the X-ray diffraction patterns are all similar and typical of the mesomorphic form,[4,5] as shown, for instance, in the sample with η = 0.8 dL/g, by flat plate photograph of Figure 5(A). For the same sample, the equatorial scan and the azimuthal scan, relative to the meridional reflection on the third layer line collected by an automatic diffractometer, are reported in Figures 6(A) and 7(A), respectively. The scan that is relative to the meridional reflection on the third layer line is preferred over the analogous scans that are relative to the other meridional reflections of the mesomorphic structure, on the first and fifth layer lines. In fact, the meridional reflection on the first layer line is weak and that reflection on the fifth layer line is too close to a nearly meridional reflection of the triclinic structure [the ($\bar{1}05$) presents an azimuthal displacement from the meridian of nearly 10°].[6] The presence of a meridional reflection on the third layer line [Fig. 7(A)] and of only a broad diffraction peak on the equator [Fig. 6(A)] clearly indicates the presence of the mesomorphic phase of PET.

The birefringence, which for the as-spun fibers is in the range 0.006–0.02 (Fig. 4), increases for all the drawn samples, independently of the molar mass, to 0.16 ± 0.01. This birefringence value is close to those reported for PET amorphous samples (films and fibers) that were drawn in the temperature range 20–60°C.[18,21,39] Hence, the molecular orientation increases with the molar mass for the spinning process (which involves the melt state), while it is unaffected for the drawing process at room temperature (which involves the solid state).

The DSC scan of a mesomorphic fiber, drawn at

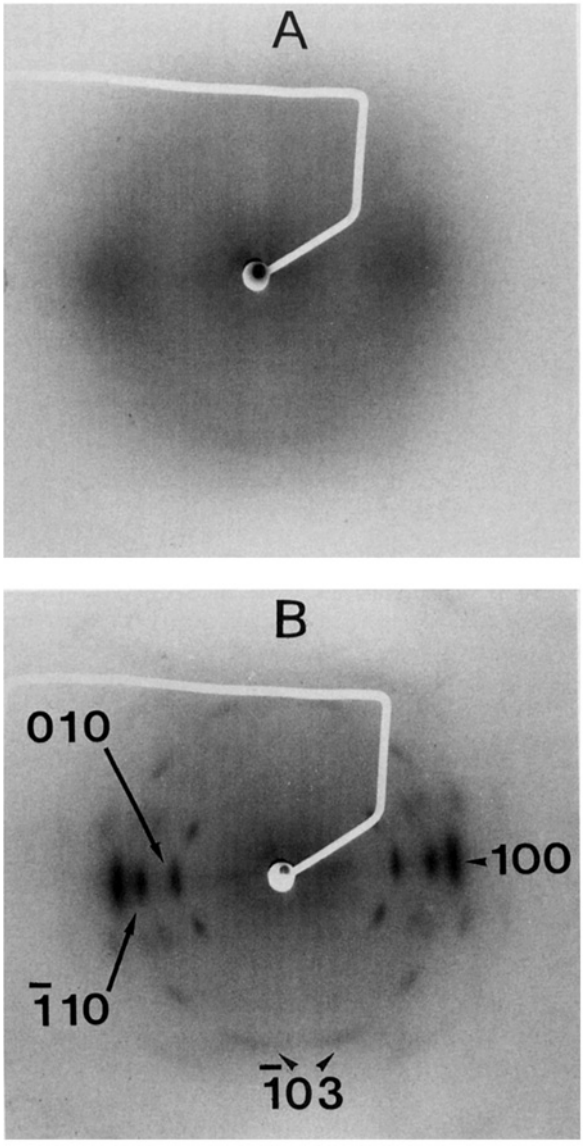

Figure 5 X-ray diffraction flat plate photographs for the mesomorphic fiber, with $\eta = 0.8$ dL/g, (A) unannealed, and (B) after annealing for 15 min at 180°C. The Miller indexes of those reflections on the equator and the third layer line, recorded through an automatic diffractometer [see Figs. 6(D) and 7(D)], are indicated.

room temperature ($\eta = 0.8$ dL/g), is compared in Figure 8 with the DSC scan of the corresponding amorphous as-spun fiber. As described in the literature for analogous PET samples, drawn at temperatures below the glass transition,[15–19] a broad and complex exothermic peak is present [Fig. 8(B)]. This exothermic peak, which for our fibers is located in the temperature range 60–150°C and has a maximum nearly at 85°C, is spanned in a temperature range in which both phenomena of glass transition

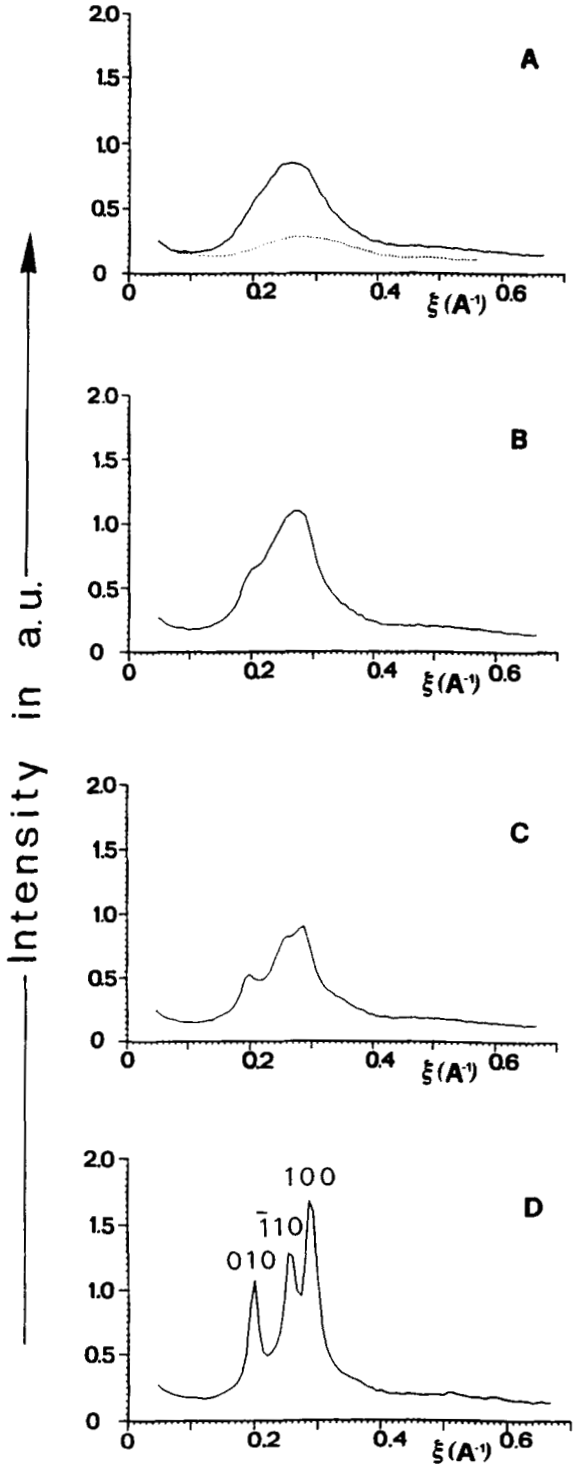

Figure 6 X-ray diffraction equatorial scans for the mesomorphic fiber, with $\eta = 0.8$ dL/g, annealed for 15 min at different temperatures: (A) unannealed, (B) 60°C, (C) 80°C, and (D) 180°C. The intensities are in arbitrary units (a. u.). The dotted line in Figure 6(A) represents the diffraction by the glass capillary used for the measurement. In Figure 6(D), the Miller indexes of equatorial reflections of PET in the triclinic form are indicated.

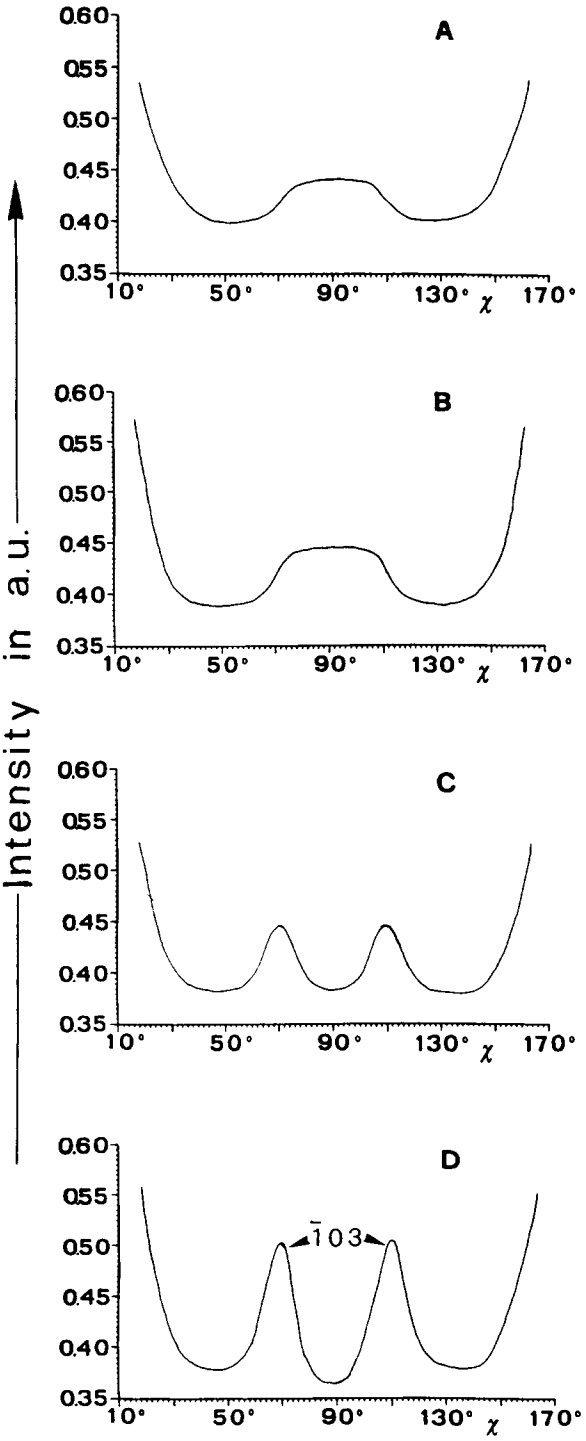

Figure 7 X-ray diffraction azimuthal scans at 2Θ, corresponding to the maximum diffraction intensity on the third layer line, for the mesomorphic fiber with η = 0.8 dL/g, annealed for 15 min at different temperatures: (A) unannealed (2Θ = 25.8°), (B) 60°C (2Θ = 25.8°), (C) 80°C (2Θ = 26.6°), and (D) 180°C (2Θ = 26.6°). The intensities are in arbitrary units (a. u.). In Figure 7(D), the Miller indexes of the reflection, on the third layer line of PET in the triclinic form, are indicated.

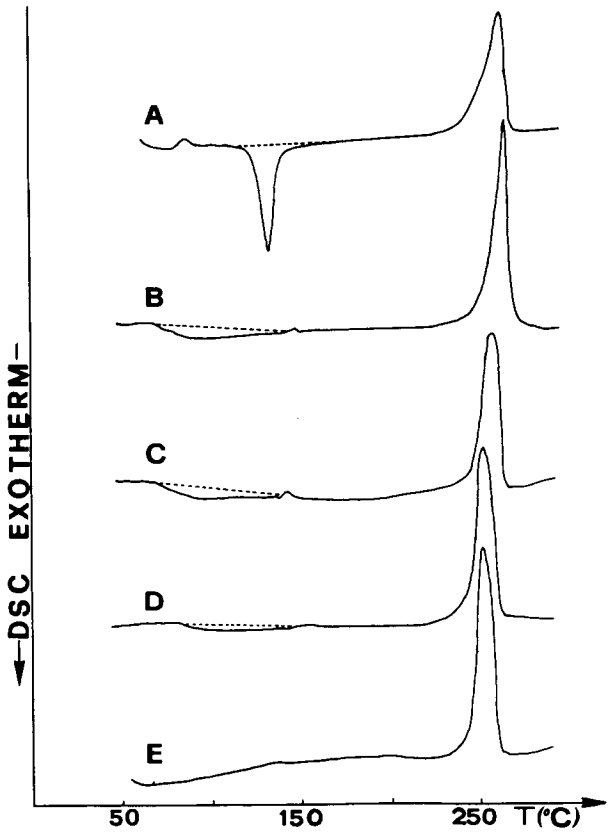

Figure 8 DSC scans for the fiber with η = 0.8 dL/g: (A) amorphous [taken from Fig. 1(B)] and mesomorphic, annealed for 15 min at different temperatures, (B) unannealed, (C) 50°C, (D) 80°C, and (E) 180°C. Dashed lines point out the considered exothermic peaks (see text).

and crystallization should occur. Due to the broadness of the exothermic peak and to the possible superposition with the glass transition, the crystallization enthalpy (ΔH_c) cannot be evaluated accurately. Its value is, however, not far from 15 J/g, in qualitative agreement with the ΔH_c values measured for PET films drawn at temperatures below the glass transition (Fig. 8 in Ref. 16 and Fig. 11 in Ref. 18). The crystallization enthalpy for the mesomorphic samples is hence smaller than for the amorphous spun fibers ($\Delta H_c \approx$ 25 J/g for all the scans in Fig. 1).

A comparison of the melting endothermic peaks for all the amorphous and mesomorphic fibers of different molar masses [for instance, for the melting peaks of Figs. 8(A) and (B)] shows that for the mesomorphic drawn samples of the peaks are narrower (e.g., the half width is $\approx$ 9°C rather than $\approx$ 11°C), are more intense (the melting enthalpy increases from nearly 40 J/g to nearly 50 J/g), and are located at higher temperatures (at nearly 257°C rather than at 253–254°C). This indicates that

higher crystalline perfections and degrees of crystallinity are reached, upon crystallization at the heating conditions of the DSC scans, from the highly oriented mesomorphic fibers, rather than from the poorly oriented amorphous samples. Assuming that the melting enthalpy of a fully crystalline PET sample is 140 ± 20 J/g,[40] the degrees of crystallinity reached in the conditions of the DSC scans are nearly 28% for the amorphous fibers and nearly 36% for the mesomorphic fibers.

The glass transition and the crystallization phenomena are better resolved by the dynamic-mechanical analysis. The DMA scan for a mesomorphic monofilament (η = 0.8 dL/g) is reported, for instance, in Figure 9(A). Strictly analogous scans are obtained for the other mesomorphic monofilaments or for bundles of fibers of different molar masses.

In the temperature range 60–150°C, the loss factor tan δ presents two broad, but well defined peaks. The peak at higher temperature is easily attributed to the glass transition of the semicrystalline sample, generated by the scan. In fact, the main drop of the elastic modulus is correspondingly observed. The large increases of the glass transition temperature

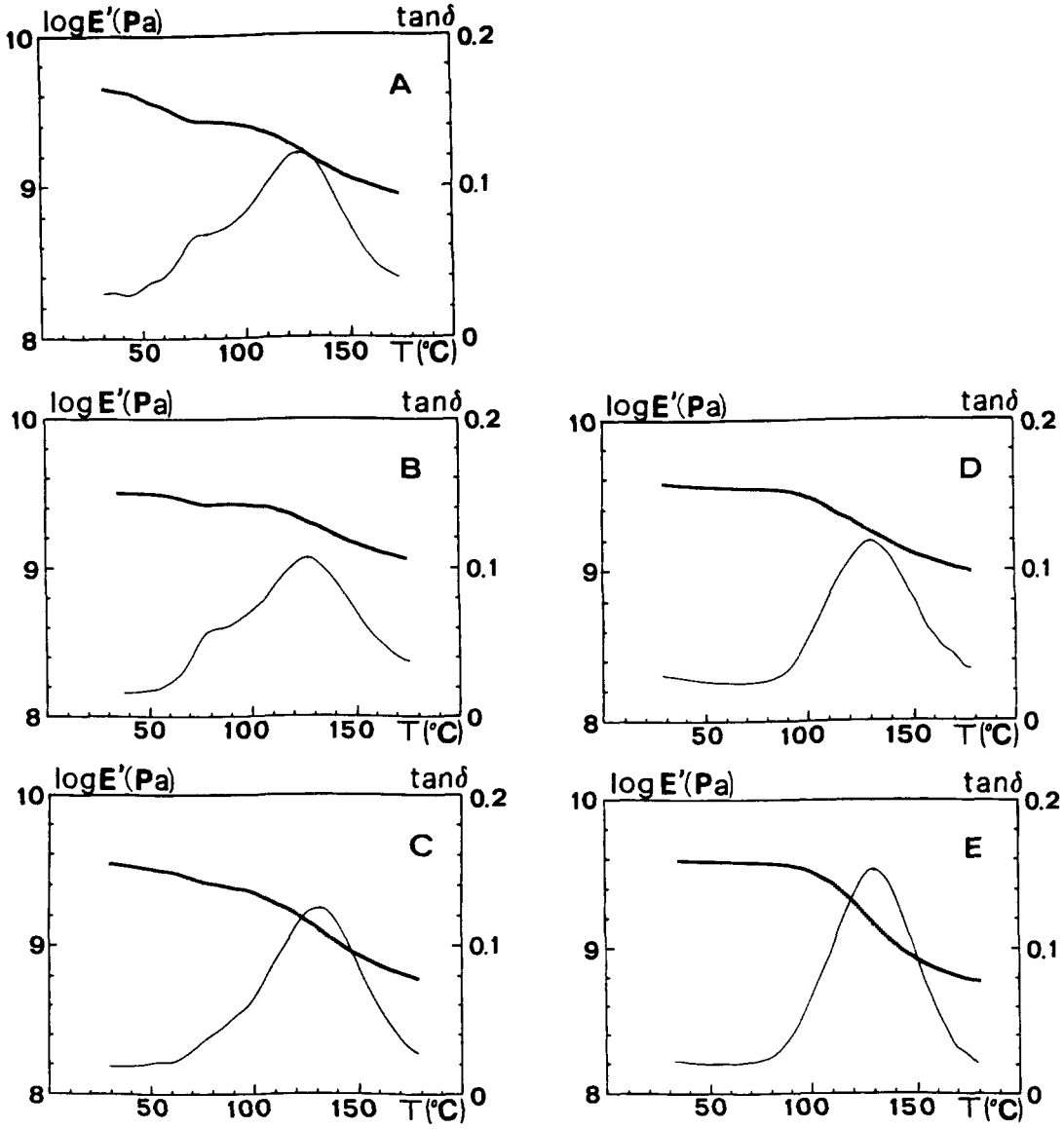

Figure 9 Storage modulus (E', thick solid line) and loss factor (tan δ, thin solid line), from dynamic mechanical measurements, for the room temperature drawn monofilaments, with η = 0.8 dL/g, annealed for 15 min at different temperatures: (A) unannealed, (B) 40°C, (C) 60°C, (D) 80°C, and (E) 180°C.

for crystalline oriented samples of PET, with respect to the amorphous as well as crystalline unoriented samples, is described in the literature.[41,42]

More complex is the attribution of the lower temperature tan δ peak, which for all the considered mesomorphic samples is in the range 75–80°C. This could be attributed to the sum of two phenomena. In the temperature range 50–100°C, the elastic modulus presents an initial drop (possibly associated with the glass transition of the sample not yet crystalline), followed by a small reclimbing (associated with the crystallization from the mesomorphic form).* The present attribution of both tan δ peaks is also confirmed by the DMA analyses on crystalline fibers that are obtained by annealing procedures on the mesomorphic samples (as shown in the next section).

Annealed Mesomorphic Fibers

In this section, in order to study the crystallization from the mesomorphic phase, mesomorphic fibers annealed with fixed ends at different temperatures have been characterized.

The annealing procedures at constant length of the mesomorphic fibers, which gradually produce crystallization into the triclinic form, do not change substantially the stress–strain behavior for all the fibers, regardless of the value. Hence, as for the mesomorphic fibers of the previous section, higher modulus and tenacity are observed for the semicrystalline fibers of higher molar mass. This behavior, not yet reported for mesomorphic samples, has been instead well described for semicrystalline samples.[11,44,45]

All the results presented in the following are substantially independent of η, hence only the results relative to the fiber with $\eta = 0.8$ dL/g are reported.

The equatorial scans of the X-ray diffraction patterns for the mesomorphic fiber annealed at 60, 80, and 180°C are shown in Figures 6(B), (C), and (D), respectively. The azimuthal scans at 2Θ of 25.8° or 26.6° (corresponding to the maximum diffraction intensity on the third layer line), for the fiber annealed at the same temperatures, are shown in Figures 7(B), (C) and (D), respectively. The pattern of the fiber annealed at 60°C, at variance with the pattern of the fiber annealed at 40°C (not reported), which is still typical of a mesomorphic form, presents on the equator a halo with shoulders corresponding to the main reflections of the triclinic crystalline form. All these peaks, as well as the peaks on the third layer line with indexes $(\bar{1}03)$,[6] are clearly developed in the fibers annealed at 80°C [Figs. 6(C) and 7(C)] and at 180°C (Figs. 6(D) and 7(D)]. For comparison, the flat plate photograph for the sample annealed at 180°C is shown in Figure 5(B) [the Miller indexes of the reflections, which are present in the diffraction profiles of Figs. 6(D) and 7(D), are indicated).

For the mesomorphic fiber, annealed at 80°C, the X-ray diffraction azimuthal scans, at different 2Θ values in the range 25°–27°, do not show any meridional reflection. It is, hence, reasonable to conclude that, in the sample annealed at 80°C, the mesomorphic phase has been substantially transformed into a triclinic crystalline phase.

The increase of the areas and the sharpening of the peaks, typical of the triclinic form, by annealing at higher temperatures [e.g., see Figs. 6(D) and 7(D)], would therefore correspond to an increase in the degree of crystallinity (possibly at the expense of the amorphous phase) and in the size and perfection of the crystallites.

The DSC scans of the fibers, annealed at different temperatures, reported in Figures 8(C–E), show that the broad exothermic peak of the mesomorphic sample gradually disappears by annealing procedures up to 180°C. However, well defined exothermic peaks are still present in annealed samples for which the mesomorphic phase has been already disappeared. For instance, for the drawn samples annealed at 80°C, the enthalpy of crystallization is still equal to $\approx$ 5 J/g (the corresponding value for the unannealed sample is $\approx$ 15 J/g).

The graduality of the increase in the degree of crystallinity by annealing procedures at increasing temperatures up to 200°C, for PET samples drawn at room temperature, has been clearly shown also by previous specific volume measurements (Figs. 2 and 3 in Ref. 17).

The birefringence of the annealed fibers increases from 0.16 ± 0.01 to 0.19 ± 0.01 (also, in this case, substantially independently of the molar mass) for annealing procedures in the range 80°C–120°C. The increase of the birefringence with the annealing temperature (and hence with the crystallization) is in this case smaller than the increase observed for annealing procedures on less oriented amorphous PET fibers that are spun at high speeds (e.g., from 0.06 to 0.15 in Ref. 46).

Some DMA scans of drawn and annealed monofilaments are shown in Figure 9. The low tempera-

* The cryogenic relaxations for PET samples drawn below T_g (hence mesomorphic), as well as for drawn samples annealed at 200°C (crystallized), have been studied by dynamic mechanical measurements.[43]

ture tan δ peak of the mesomorphic form [Fig. 8(A)] tend to disappear for annealing procedures above 40°C. In particular, the peak is present as a shoulder in the pattern of the sample annealed at 60°C [Fig. 9(C)] and is completely absent in the samples annealed at 80°C [Fig. 9(D)] and 180°C [Fig. 9(E)].

These data clearly confirm the attribution of both tan δ peaks of the mesomorphic samples (presented in the previous section). That is, the low temperature peak is related to the glass transition of the starting material, which is promptly followed by crystallization from the mesomorphic form to the triclinic crystalline form; the high temperature peak is related to the glass transition temperature of the semicrystalline sample that was generated by the temperature scan.

CONCLUSIONS

The molar mass of the PET samples can have a large influence on the properties of the as-spun samples. In particular, for samples spun in identical industrial conditions (temperature speeds, etc.), well defined differences in the crystallization temperature (as pointed out by DSC and DMA analyses) and in the molecular degree of orientation (birefringences) have been shown.

For samples subsequently drawn at room temperature (mesomorphic), as well as for the same samples also annealed at temperatures up to 180°C (crystalline), the different molar masses correspond to large differences in the tensile elastic modulus and strength. However, correspondingly, the crystalline structure, revealed by X-ray diffraction patterns, the orientation as measured by birefringence measurements, and the crystallization temperatures, as shown by DSC and DMA scans, are scarcely dependent on the polymer molar mass.

For the mesomorphic samples in the DSC scans, a broad and complex exothermic peak is present, spanning a temperature range (50–150°C) in which glass transition and crystallization phenomena should occur. The glass transition and the crystallization phenomena are better resolved by dynamic-mechanical analysis. The DMA data (in the same temperature range) of the mesomorphic samples can be interpreted by a succession of three main phenomena: glass transition of the starting material (mesomorphic oriented), crystallization from the mesomorphic to the crystalline form, and glass transition of the semicrystalline oriented sample generated by the temperature scan.

The X-ray diffraction analysis of mesomorphic samples, annealed at different temperatures, mainly based on azimuthal scans relative to the meridional peak on the third layer line, indicates that for all the considered drawn samples, the mesomorphic phase substantially disappears for annealing at 80°C. The broad exothermic peaks, which are still present in the DSC scans of the samples annealed at 80°C or 100°C, as well as the gradual decrease of the specific volume for annealing up to 200°C,[17] are therefore due only to a gradual increase in the degree of crystallinity (at expenses of the amorphous phase) and in the size and perfection of the crystallites.

The authors wish to thank Prof. P. Corradini and Prof. C. De Rosa of the University of Naples for many useful discussions. This work was supported by the Ministero dell'Universitá della Ricerca Scientifica e Tecnologica, Italy, and by the Consiglio Nazionale delle Ricerche. X-ray diffraction data were recorded with a Nonius CAD4 automatic diffractometer (Centro Interdipartimentale di Metodologie Chimico Fisiche, University of Naples).

REFERENCES

1. R. Bonart, *Kolloid-Z.*, **213,** 1 (1966).
2. R. Bonart, *Kolloid-Z.*, **210,** 16 (1966).
3. R. Bonart, *Kolloid-Z.*, **231,** 438 (1968).
4. T. Asano and T. Seto, *Polym. J.*, **5,** 72 (1973).
5. F. Auriemma, P. Corradini, C. De Rosa, G. Guerra, V. Petraccone, R. Bianchi, and G. Di Dino, *Macromolecules,* **25,** 2490 (1992).
6. R. P. Daubeny, C. W. Bunn, and C. Brown, *J. Proc. R. Soc. London,* **A226,** 531 (1954).
7. I. H. Hall, In: *Structure of Crystalline Polymers,* I. H. Hall, Ed., Elsevier, London, 1984, Chap. 2, p. 39.
8. A. Misra and R. S. Stein, *J. Polym. Sci. Polym. Phys. Ed.*, **17,** 235 (1979).
9. M. Amano and K. Nakagawa, *Polymer,* **27,** 1559 (1986).
10. K. Itoyama, *J. Polym. Sci. Polym. Lett.*, **25,** 331 (1987).
11. M. Ito, K. Tanaka, and T. Kanamoto, *J. Polym. Sci. Polym. Phys. Ed.*, **25,** 2127 (1987).
12. M. Matsuo and C. Sawatari, *Polym. J.*, **22,** 518 (1990).
13. S. Fakirov and M. Evstatiev, *Polymer,* **31,** 431 (1990).
14. M. Ito, K. Takahashi, and T. Kanamoto, *J. Appl. Polym. Sci.*, **40,** 1257 (1990).
15. M. Ito, K. Takahashi, and T. Kanamoto, *Polymer,* **31,** 58 (1990).
16. S. D. Long and I. M. Ward, *J. Appl. Polym. Sci.*, **42,** 1911 (1991).
17. V. Busico, P. Corradini, F. Riva, A. Seves, and L. Vicini, *Makromol. Chem. Rapid Commun.*, **1,** 423 (1980).

18. G. Hinrichsen, H. G. Adam, H. Krebs, and H. Springer, *Colloid & Polym. Sci.*, **258,** 232 (1980).
19. T. Sun, J. Pereira, and R. S. Porter, *J. Polym. Sci. Polym. Phys. Ed.*, **22,** 1163 (1984).
20. H. Springer, U. Brinkmann, and G. Hinrichsen, *Colloid & Polym. Sci.*, **259,** 38 (1981).
21. M. J. Napolitano and A. Moet, *J. Appl. Polym. Sci.*, **34,** 1285 (1987).
22. S. A. Jabarin and E. A. Lofgren, *Polym. Eng. Sci.*, **26,** 620 (1986).
23. R. Bianchi, P. Chiavacci, R. Vosa, and G. Guerra, *J. Appl. Polym. Sci.*, **43,** 1087 (1991).
24. E. A. Turi, *Thermal Characterization of Polymeric Materials*, Academic, New York, 1981, p. 771.
25. A. B. Thompson and D. W. Woods, *Trans. Faraday Soc.*, **52,** 1383 (1956).
26. K. H. Illiers and H. Breuer, *J. Colloid Sci.*, **18,** 1 (1963).
27. J. H. Dumbleton and T. Murayama, *Kolloid Z. Z. Polym.*, **41,** 220 (1967).
28. J. P. Bell and T. Murayama, *J. Polym. Sci. Part A-2,* **1,** 1059 (1969).
29. V. Frosini and A. E. Woodward, *J. Macromol. Sci. Phys.*, **B3,** 91 (1969).
30. K. K. Mocherla and P. Bell, *J. Polym. Sci. Polym. Phys. Ed.*, **11,** 1779 (1973).
31. R. E. Metha and J. P. Bell, *J. Polym. Sci. Polym. Phys. Ed.*, **11,** 1793 (1973).
32. D. F. Fagerburg, *J. Appl. Polym. Sci.*, **30,** 889 (1985).
33. J. H. Dumbleton and T. Murayama, *J. Appl. Polym. Sci.*, **14,** 2921 (1970).
34. B. Gumther and H. G. Zachmann, *Polymer,* **24,** 1008 (1983).
35. F. S. Smith and R. S. Steward, *Polymer,* **15,** 283 (1974).
36. G. C. Alfonso, M. P. Verdona, and A. Wasiak, *Polymer,* **19,** 711 (1978).
37. G. Althen and H. G. Zachmann, *Makromol. Chem.,* **180,** 2723 (1979).
38. P. Desai and A. S. Abhiraman, *J. Polym. Sci. Polym. Phys. Ed.*, **23,** 653 (1985).
39. F. Rietsch, R. A. Duckett, and A. Ward, *Polymer,* **21,** 1133 (1979).
40. A. Metha, H. Gaur, and B. Wunderlich, *J. Polym. Sci. Polym. Phys. Ed.*, **16,** 289 (1978).
41. D. W. Woods, *Nature,* **174,** 753 (1954).
42. J. H. Dumbleton, T. Murayama, and J. P. Bell, *Kolloid Z.-Z. Polym.*, **54,** 228 (1968).
43. C. D. Armeniades and E. Baer, *J. Polym. Sci. Part A-2,* **9,** 1345 (1971).
44. K. W. Hillier, *Man-Made Fibres Science and Technology,* Interscience, Chichester, 1968, Vol. 3, p. 12.
45. P. Bouriot, In: *Fibre Reinforcements for Composite Materials,* A. R. Bensell, Ed., Elsevier, Amsterdam, 1988, p. 331.
46. K. M. Gupte, H. Motz, and J. M. Schultz, *J. Polym. Sci. Polym. Phys. Ed.*, **21,** 1927 (1983).

Received April 2, 1993
Accepted September 27, 1993